Impact of skeletal dissolution and secondary aragonite on trace element and isotopic climate proxies in *Porites* corals

E. J. Hendy,[1] M. K. Gagan,[2] J. M. Lough,[3] M. McCulloch,[2] and P. B. deMenocal[4]

Received 30 March 2007; revised 19 July 2007; accepted 30 July 2007; published 5 October 2007.

[1] Restricted zones of recent dissolution and secondary aragonite infilling were identified in a coral core collected in 1986 from a living massive *Porites* colony from the central Great Barrier Reef, Australia. Secondary aragonite needles, $\geq$20 μm long, cover skeletal surfaces deposited from 1972 to late 1974 and increase bulk density by 10%. Dissolution is observed above this zone, whereas older skeleton is pristine. We investigate the impact of both types of early marine diagenesis on skeletal geochemistry and coral paleoclimate reconstructions by comparison with similar records from eight contemporary *Porites* colonies collected at nearby reefs. Secondary aragonite overgrowth causes anomalies in skeletal density, Mg/Ca, Sr/Ca, U/Ca, δ^{18}O, and δ^{13}C. The secondary aragonite is consistently associated with a cool temperature anomaly for each of the sea surface temperature (SST) proxies (δ^{18}O-SST -1.6°C; Sr/Ca-SST -1.7°C; Mg/Ca-SST -1.9°C; U/Ca-SST -2.8°C). Dissolution, through incongruent leaching, also causes cool SST artifacts but only for trace element ratios (Mg/Ca-SST -1.2°C; Sr/Ca-SST -1.2°C; U/Ca-SST -2.1°C). The sequence of preference with respect to dissolution of coral skeleton in seawater is Mg > Ca > Sr > U. Rigorous screening of coral material for paleoclimate reconstructions is therefore necessary to detect both dissolution and the presence of secondary minerals. The excellent agreement between apparent SST anomalies generated by different modes of diagenesis means that replication of tracers within a single coral cannot be used to validate climate-proxy interpretations. Poor replication of records between different coral colonies, however, provides a strong indication of nonclimatic artifacts such as dissolution and secondary aragonite.

Citation: Hendy, E. J., M. K. Gagan, J. M. Lough, M. McCulloch, and P. B. deMenocal (2007), Impact of skeletal dissolution and secondary aragonite on trace element and isotopic climate proxies in *Porites* corals, *Paleoceanography*, *22*, PA4101, doi:10.1029/2007PA001462.

1. Introduction

[2] The aragonite skeletons of long-lived massive corals like *Porites* sp. are valuable archives of past tropical climates and environments. For example, coral skeletons incorporate a range of isotopic (δ^{18}O) and elemental (Sr/Ca, U/Ca, Mg/Ca) tracers that can provide subannually resolved reconstructions of sea surface temperature (SST; reviewed by *Gagan et al.* [2004]). Aragonite is, however, metastable in the marine environment. Early diagenesis can occur as dissolution and/or infilling of vacated skeleton with secondary aragonite [*Constantz*, 1986]. In this paper we show, for the first time, that both dissolution and secondary aragonite influence a wide range of tracers that are commonly measured in coral skeletons (density, δ^{13}C, δ^{18}O, Sr/Ca, U/Ca, and Mg/Ca). The two forms of diagenesis, however, cause different artifacts in the paleoclimate record.

[3] Previous research has shown that early marine diagenesis influences coral skeletal geochemistry [e.g., *Bar-Matthews et al.*, 1993; *Enmar et al.*, 2000; *Lazar et al.*, 2004; *Müller et al.*, 2001, 2004; *Quinn and Taylor*, 2006]. Positive anomalies were identified in diagenetically altered *Porites* sp. skeletons containing secondary aragonite overgrowth for Sr/Ca [*Castellaro et al.*, 1999; *Enmar et al.*, 2000; *Müller et al.*, 2001; *Quinn and Taylor*, 2006], U/Ca [*Castellaro et al.*, 1999; *Lazar et al.*, 2004], δ^{18}O [*Castellaro et al.*, 1999; *Enmar et al.*, 2000; *Müller et al.*, 2001] and δ^{13}C [*Müller et al.*, 2004], and negative anomalies for Mg and Mg/Ca [*Bar-Matthews et al.*, 1993; *Enmar et al.*, 2000; *Quinn and Taylor*, 2006]. As a result there has been a call to screen all coral used to reconstruct paleoclimate records for secondary aragonite overgrowth [*Gagan et al.*, 2004].

[4] In contrast to secondary aragonite, the geochemical impact of coral skeletal dissolution has received little attention, and its effect on coral-based climate reconstructions has remained untested. Yet, resolving the question of whether dissolution in the marine environment alters the coral-based elemental and isotopic paleoclimate records is of increasing importance because of the anticipated increase in ocean acidification due to higher atmospheric CO_2 levels and resulting exposure of coral archives to greater dissolution. Early laboratory-based experiments indicated that dissolution could cause geochemical anomalies, but the

[1]Department of Earth Sciences, University of Bristol, Bristol, UK.
[2]Research School of Earth Sciences, Australian National University, Canberra, ACT, Australia.
[3]Australian Institute of Marine Science, Townsville MC, Queensland, Australia.
[4]Lamont-Doherty Earth Observatory of Columbia University, Palisades, New York, USA.

0883-8305/07/2007PA001462$12.00

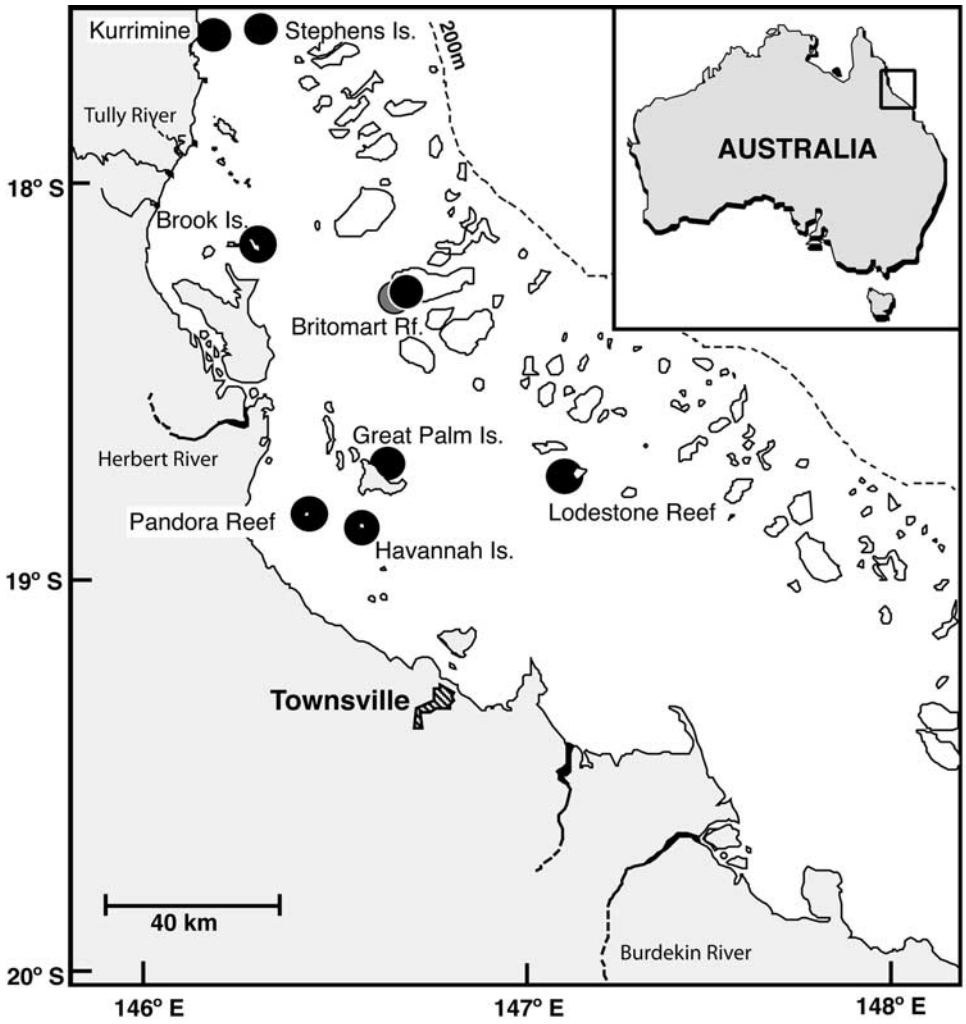

Figure 1. *Porites* colony sample sites in the central Great Barrier Reef, Australia. Zones of dissolution and secondary aragonite deposition were found in the Great Palm Island core.

results were contradictory due to the low precision techniques available at the time (i.e., AA spectroscopy). *Schroeder* [1969] reported that aragonite powder exposed to seawater for a period of 120 days dissolved incongruently with respect to Mg, Ca, and Sr (i.e., these elements dissolve in proportions different from those in the original solid). The sequence of preference with respect to dissolution in seawater was Mg > Ca > Sr [*Schroeder*, 1969]. *Amiel et al.* [1973] also found incongruent dissolution for Mg/Ca but reported congruent dissolution for Sr/Ca. Recently, incongruent dissolution of Mg, Sr, and Na relative to Ca from powered coral aragonite has been observed in laboratory-based, freshwater-leaching experiments [*Fairchild and Killawee*, 1995; I. J. Fairchild, personal communication, 2006]. In this study we undertake the first test of whether dissolution affects the geochemistry of an intact coral skeleton under marine conditions.

[5] We isolate the geochemical overprint of both types of early marine diagenesis by focusing on restricted zones of dissolution and secondary aragonite that occurred within the skeleton of a living *Porites* colony. The diagenesis occurred extremely rapidly, within a decade of the coral tissue vacating the section of skeleton. We examine the impact of incongruent dissolution and secondary aragonite on coral climate reconstructions by comparison with contemporary stable isotope and trace element records measured from a control population of unaltered *Porites* colonies. This approach is different from previous studies that have typically focused on the offset caused by contamination from secondary aragonite by comparing primary coral aragonite and adjacent secondary aragonite overgrowth or bulk mixtures of the two within a specimen.

2. Material and Methods

[6] Nine massive *Porites* coral cores or whole colonies were collected from reefs within a 60 km radius in the central Great Barrier Reef, Australia between 1984 and 1989 (Figure 1) [*Lough et al.*, 1999]. Slices from the coral skeletons were prepared and cross-dated as described by *Hendy et al.* [2003], and powders milled for three to five common 5-year periods starting and ending in the winter

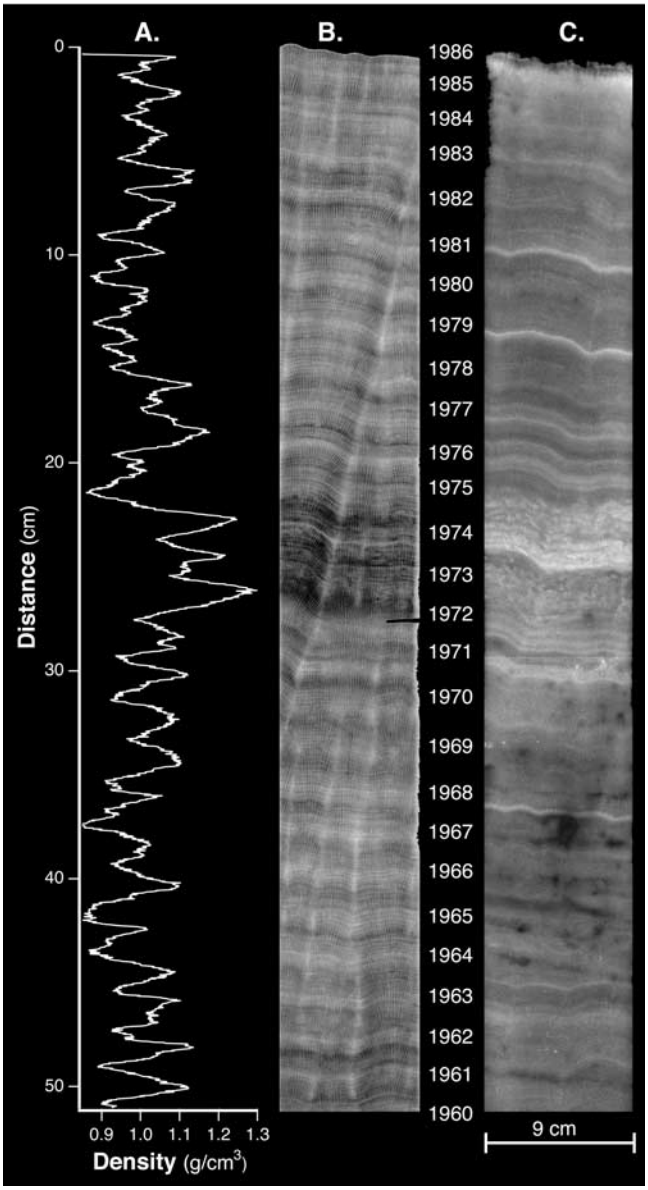

Figure 2. (a) Densitometry track, (b) X-radiograph positive print, and (c) UV luminescence photograph of Great Palm Island core section (1960–1986). Overgrowth of secondary aragonite occurs between 1972 and late 1974; note the associated increase in density and bright mottled luminescence.

dry season for 1955–1960, 1960–1965, 1965–1970, 1970–1975, and 1975–1980 [*Hendy et al.*, 2002].

[7] Skeletal density was measured by gamma densitometry along the vertical growth axis of each coral slice (e.g., Figure 2a) [*Lough and Barnes*, 1997, 2000]. Coral slices were photographed under UV light onto black and white film to reveal luminescent banding (Figure 2c) [*Hendy et al.*, 2003]. Scanning electron microscope images (Figure 3) were collected using a Cambridge S360 on gold-coated slivers cut longitudinal to the growth axis. Stable isotopes were analyzed in duplicate on powders reacted in a Kiel device on a Finnigan MAT 251. Average standard deviation (sd) of NBS-19 analyzed six times per 24 hour run was 0.04‰ for $\delta^{18}O$ and 0.02‰ for $\delta^{13}C$ (n = 281; over 3 years). The average sd between duplicate coral samples (n = 449) was 0.04‰ for $\delta^{18}O$ and 0.03‰ for $\delta^{13}C$.

[8] Sr/Ca ratios were determined by isotope dilution using a mixed ^{43}Ca-^{84}Sr spike and analyzed on a Finnigan MAT 261 TIMS [*Alibert and McCulloch*, 1997]. The average sd between duplicated samples was 0.005 mmol/mol (n = 125; over 3 years). An aliquot of the sample solution used for the Sr/Ca measurement was analyzed for U/Ca using a mixed spike of ^{45}Sc (as a proxy for ^{45}Ca) and ^{235}U and measurement on a Fisons PlasmaQuad II ICP-MS (1sd = 0.012 μmol/mol, n = 18 duplicates).

[9] Two sets of Mg/Ca measurements were made for each sample: "untreated" and "treated." The "treated" powder subsamples were exposed to a mixture of H_2O_2 and NaOH and then leached with a weak HNO_3 solution according to methods outlined for cleaning foraminifera for Mg/Ca [*Boyle and Keigwin*, 1985; *Boyle and Rosenthal*, 1996]. This treatment is similar to *Mitsuguchi et al.*'s [2001] suggestion for cleaning coral for Mg/Ca, with the exception that the oxidation step is buffered. "Untreated" subsamples were run to determine the effect of the cleaning treatment. Ca, Mg, and Sr concentrations were measured on a Jobin Yvon ICP-AES, with the raw data drift corrected as described by *Schrag* [1999]. Average sd of Mg/Ca sample splits was ±0.048 mmol/mol. Mg/Ca measurements were not made for the period 1955–1960.

3. Results

3.1. Visual Evidence of Diagenesis

[10] Early diagenesis is visible in the X-ray positive (Figure 2b), UV photographs (Figure 2c), and SEM images (Figure 3) of the coral core (GPI Ø2A-Ø1) collected from a living colony at Great Palm Island in 1986. SEM was used to positively identify the dissolution and secondary aragonite zones along a transect down the coral core. Secondary aragonite infilling is concentrated in skeleton laid down between 1972 and late 1974 (Figures 3a and 3b). Aragonite needles, $\geq$20 μm long, cover all skeletal surfaces with the exception of the basal surface of dissepiments. In contrast, older skeleton below this zone is pristine (Figures 3c and 3d). Evidence of dissolution is seen in the skeleton directly above the zone of secondary aragonite (Figures 3e–3h), and extends over the period 1975 to mid-1978 with a gradient of lessening dissolution toward the more recent material. The boundary between the two zones is very clear (Figures 3g and 3h) and follows a dissepiment. Within the dissolution zone the skeletal surface is strongly etched which exposes individual aragonite fibers within the fasciculi bundles (compare surface texture in Figures 3d and 3f). The most indicative feature of dissolution is a "melted" appearance of the crystal surfaces (e.g., center of Figure 3e). Preferential dissolution is seen along the fibers (perpendicular to the planed-off c-axis) and in pits forming within individual crystals (e.g., the fasciculi bundle shown in Figure 3f, center). A single strip of secondary aragonite overgrowth (1.5 mm), constrained within two adjacent dissepiments,

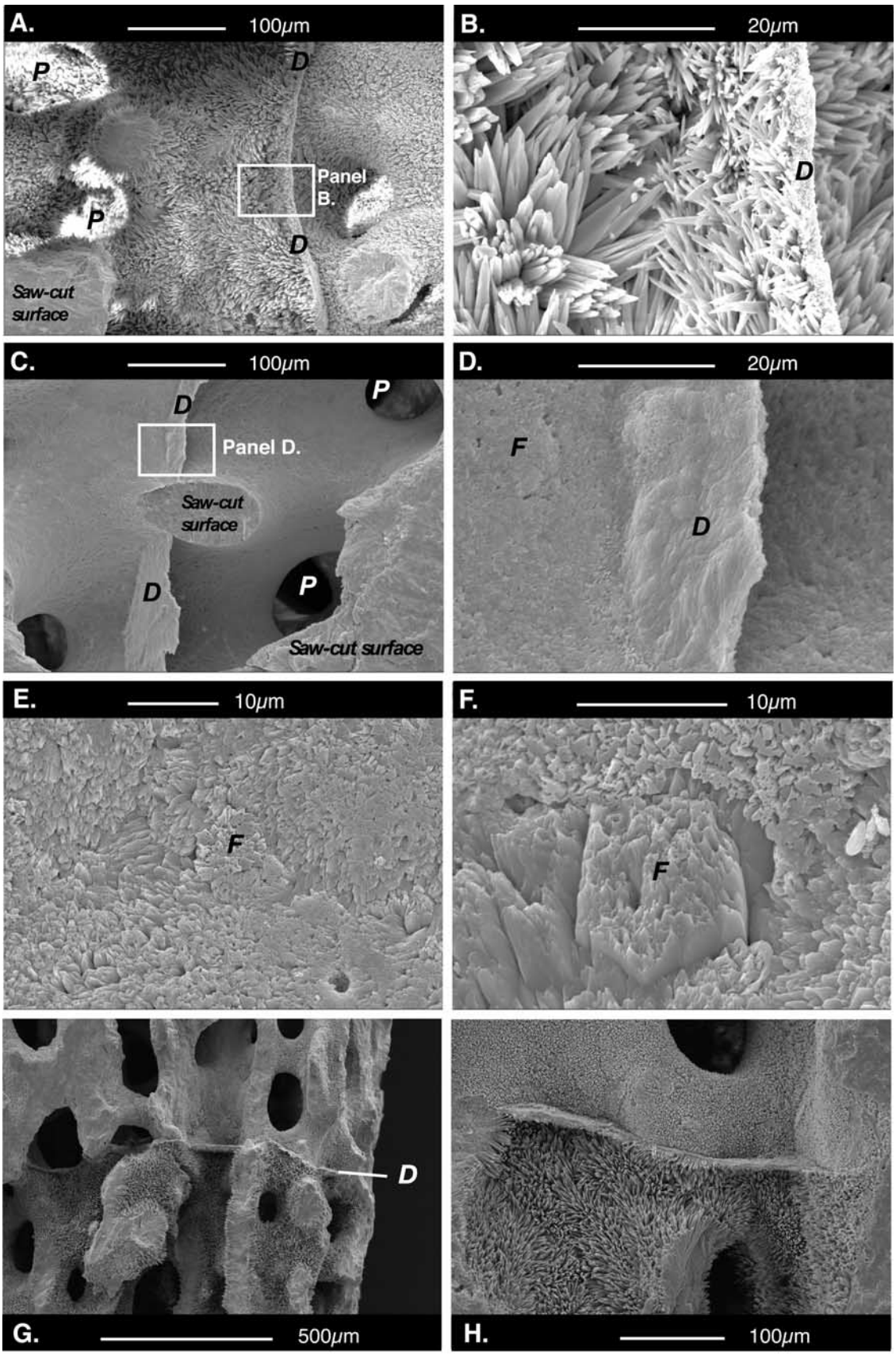
A.
100μm
P
D
Panel B.
P
D
Saw-cut surface
B.
20μm
D
C.
100μm
D
P
Panel D.
Saw-cut surface
D
P
Saw-cut surface
D.
20μm
F
D
E.
10μm
F
F.
10μm
F
D
G.
500μm
H.
100μm

Figure 3

occurs within the 67 mm section of dissolution. There was no evidence of alteration to the centers of calcification within the skeleton in either diagenetically altered zone.

[11] The Great Palm Island coral is the least dense of the nine corals studied (Figure 4a). A 10% increase in density relative to adjacent skeleton was measured for the period 1970–1975 coinciding with secondary aragonite overgrowth. The shift in skeletal density is not replicated in the contemporary records (Figure 4b). This increase in density is also visible on the X-ray positive (Figure 2). There is a suggestion in the denisitometry track of reduced skeletal density associated with the dissolution (Figure 2), but this is not large enough to affect the 5-year bulk density (Figure 4). Across both zones the subannual banding remains intact, although it is dampened in the upper section.

3.2. Geochemical Impact on Coral Climate Tracers

[12] The highest δ^{18}O and δ^{13}C, Sr/Ca, and U/Ca values and lowest Mg/Ca values for the Great Palm Island core occur in 1970–1975 (Figure 4a). Only the absolute Sr/Ca and U/Ca values appear as outliers relative to the other coral records, but when the records are compared as anomalies a strong divergence in 1970–1975 is seen for all the tracers (Figure 4b). The magnitude of the offset for the Great Palm Island core 1970–1975 mean value is +0.29‰ for δ^{18}O, +0.34‰ for δ^{13}C, +0.11 mmol/mol for Sr/Ca, and +0.13 μmol/mol for U/Ca. The Mg/Ca offset is larger prior to the cleaning treatment; the 1970–1975 mean value for the Great Palm Island core is −0.19 mmol/mol Mg/Ca relative to the control record in the ''untreated'' samples and −0.12 mmol/mol after being ''treated.'' These offsets translate into a consistent interpretation of a cool temperature anomaly, relative to the pristine coral population, of −1.6°C (δ^{18}O-SSTA), −1.7°C (Sr/Ca-SSTA), −1.9°C (Mg/Ca-SSTA ''untreated''), and −2.8°C (U/Ca-SST) (Figure 5a; using published tracer-SST calibration equations).

[13] The trace elemental ratios for the Great Palm Island core are also anomalous in the 1975–1980 dissolution zone. Sr/Ca and U/Ca values are significantly higher (+0.08 mmol/mol and +0.1 μmol/mol, respectively) and Mg/Ca lower in the ''untreated'' samples (−0.08 mmol/mol) relative to the control coral record (Figure 4b). Converted to a temperature anomaly the offset, relative to the other coral, is −1.2°C for both Sr/Ca and Mg/Ca (''untreated'') and −2.1°C for U/Ca-SSTA (Figure 5b).

[14] The cleaning process does not alter the Sr/Ca values (E. Hendy, unpublished data, 2006), but it does significantly reduce the Mg/Ca difference between the control and Great Palm Island records. In the dissolution zone this brings the ''treated'' Great Palm Island Mg/Ca values within the expected population range. The Great Palm Island coral specimen seems particularly susceptible to dissolution; samples were more vulnerable to the chemical (e.g., weak acid leach) and physical cleaning (sonication) treatments causing dramatically lower yields posttreatment. To retrieve enough ''treated'' sample for Mg/Ca analysis, twice the amount of Great Palm Island material (500 μg) needed to be processed compared with that needed for the other coral.

4. Discussion

4.1. Geochemical Impact of Incongruent Dissolution on Coral Climate Tracers

[15] This study demonstrates that dissolution impacts trace element SST proxies; the 1975–1980 Great Palm Island samples have elevated Sr/Ca and U/Ca and depleted Mg/Ca (''untreated''; Figures 4 and 5). The intact coral skeleton has dissolved incongruently in seawater with the following sequence of preferential leaching: Mg > Ca > Sr > U. The degree of incongruency [*Fairchild and Killawee*, 1995] can be expressed as the proportional change in Mg/Ca, U/Ca, and Sr/Ca relative to the expected value from the control coral population, and values range from 0.96 for Mg/Ca (''untreated''), 1.01 for Sr/Ca, and 1.08 for U/Ca. Similar behavior is evident in one Great Palm Island 1970–1975 sample, whereas a second sample on a different growth axis was normal. Possible isolated dissolution also occurred below the secondary aragonite zone, although this was not observed by SEM.

[16] There is clear evidence for selective differences in the solubility of microstructure within coral skeletons [e.g., *Constantz*, 1986]. For example, micron-scale growth zoning within aragonite fibers and centers of calcification are preferentially etched when thin sections are exposed to very weak acid [e.g., *Cuif and Dauphin*, 2004]. Recent high-resolution analysis by NanoSIMS has revealed that variations in Mg are associated with this microstructure zoning [*Meibom et al.*, 2007, and references therein]. The incongruent dissolution observed in this study may be due to the enrichment of Mg relative to Ca, Sr, and U, in more soluble zones or phases within the coral.

Figure 3. (a, b) Secondary aragonite, (c, d) pristine skeletal material, (e, f) dissolution, and (g, h) the secondary aragonite-dissolution boundary within the Great Palm Island core. The growth direction is orientated so that the youngest skeleton is on the right-hand side of Figures 3a–3f and on the top of Figures 3g and 3h. Figure 3a shows secondary aragonite overgrowth from 1972–1974 section. Secondary aragonite needles, ≥20 μm long, cover all skeletal surfaces and pores (*P*) are partially infilled with radial secondary aragonite needles. Figure 3b shows a closeup of box in Figure 3a, highlighting a dissepiment (*D*) and secondary aragonite needles. Note the secondary aragonite needles predominantly radiate from the lower surface of the dissepiment. Figure 3c shows pristine skeletal aragonite skeleton from older skeleton below the secondary aragonite zone (magnification as for Figure 3a). Note the well-preserved dissepiment (*D*) and smooth walls of the pores (*P*). Figure 3d shows pristine aragonite wall texture and dissepiment closeup from box in Figure 3c. Figures 3e and 3f show dissolution around fasciculi (*F*) bundles and within aragonite fibers in 1975–1980 Great Palm Island coral skeleton. For comparison, note smooth surfaced fasciculi in unaltered skeleton (marked ''*F*'' on Figure 3d). Figures 3g and 3h show a sharp boundary, constrained by a single dissepiment, separating the zone containing secondary aragonite overgrowth from skeleton impacted by dissolution.

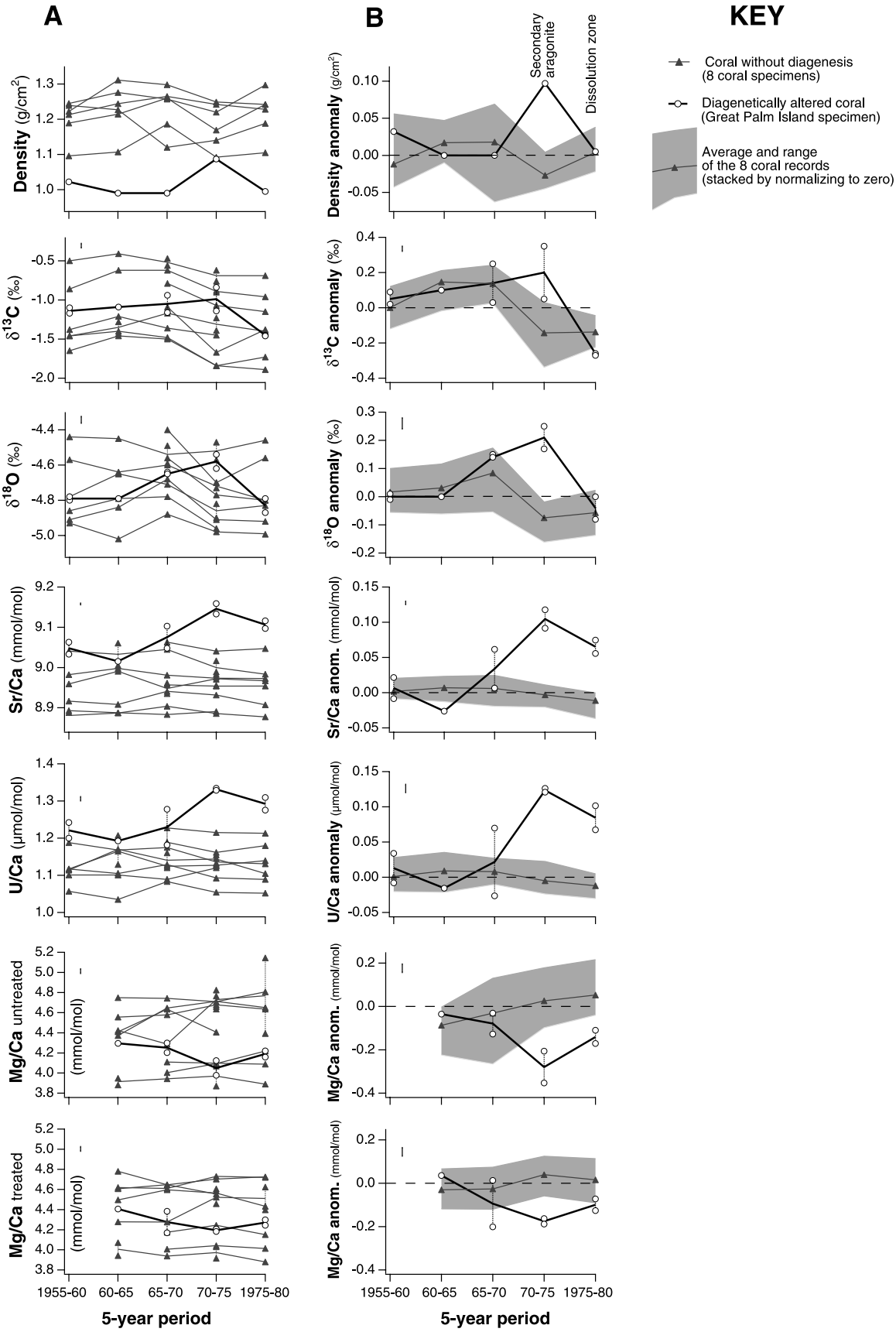
A
B
KEY
Coral without diagenesis
(8 coral specimens)
Diagenetically altered coral
(Great Palm Island specimen)
Average and range
of the 8 coral records
(stacked by normalizing to zero)
Secondary aragonite
Dissolution zone
Density (g/cm2)
Density anomaly (g/cm2)
δ13C (‰)
δ13C anomaly (‰)
δ18O (‰)
δ18O anomaly (‰)
Sr/Ca (mmol/mol)
Sr/Ca anom. (mmol/mol)
U/Ca (μmol/mol)
U/Ca anomaly (μmol/mol)
Mg/Ca untreated (mmol/mol)
Mg/Ca anom. (mmol/mol)
Mg/Ca treated (mmol/mol)
Mg/Ca anom. (mmol/mol)
1955-60
60-65
65-70
70-75
1975-80
5-year period

Figure 4

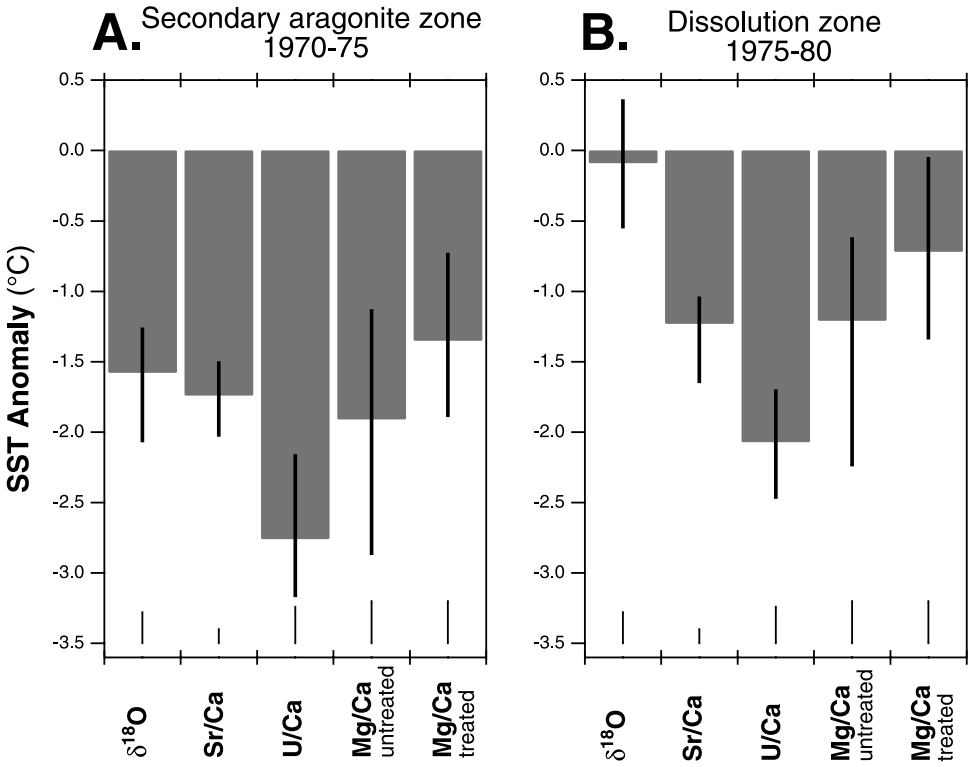

Figure 5. Apparent temperature anomalies associated with (a) secondary aragonite and (b) dissolution for each SST proxy calculated relative to the average (and range; thick line) of the stacked records for eight unaltered coral. Analytical error bars at the base of the graphs are 1σ converted into °C. The SST proxy calibration slopes used are −0.18‰ δ^{18}O per °C [*Gagan et al.*, 1998], −0.062 mmol/mol Sr/Ca per °C [*Alibert and McCulloch*, 1997], −0.0465 μmol/mol U/Ca per °C [*Min et al.*, 1995], and 0.16 mmol/mol Mg/Ca per °C [*Sinclair et al.*, 1998].

[17] Evidence from the SEM images suggests that the dissolution is occurring selectively and is dependant on the reactivity of the crystal surfaces within the coral colony skeleton (Figures 3e and 3f). Evidence that different crystallographic surfaces or crystal boundaries are dissolving at different rates can be observed in the preferential dissolution along the aragonite fibers and around fasciculi bundles. Etch pits are also forming perpendicular to the planed-off *c*-axis, probably at sites of crystal defects. It is possible that Mg is enriched, relative to Ca, Sr, and U, at a dissolution prone site along the *a*- or *b*-axis crystal edge or lattice dislocations. It is known that the edges of coral structural elements are strongly enriched in Mg [*Allison*, 1996].

[18] Early laboratory experiments on coral powder found a similar sequence of preferential leaching (Mg > Ca > Sr) [*Schroeder*, 1969] despite the difference in surfaces exposed by crushing the coral skeleton. A key question is whether the same result is found in abiotic aragonite. If true, this would make the biologically mediated microstructure of the coral skeleton irrelevant to the observed dissolution-related trace element anomalies. Pure aragonite precipitated in lab experiments dissolves congruently; however, synthetic strontianite and aragonite dissolving in $Sr(HCO_3)_2$ solutions behaves incongruently and rapidly deposit a surface phase enriched in Sr [*Plummer et al.*, 1992]. This process could explain the increase in Sr relative to Ca found in the dissolving coral skeleton, and it appears that U is also enriched in the solid solution surface phase.

[19] The process of incongruent dissolution also provides an explanation for the porewater chemistry results reported by *Enmar et al.* [2000] and *Lazar et al.* [2004] from a *Porites* colony in the Red Sea containing obvious marine

Figure 4. Coral climate tracers and density measured for each 5-year period from 1955 to 1980 in nine different coral specimens. (a) Records of absolute values of δ^{18}O, δ^{13}C, Sr/Ca, U/Ca, Mg/Ca, and density. Samples were milled for geochemical analysis along primary growth axes; adjacent growth axes were sampled to provide duplicates if material was available. (b) Records plotted as anomalies. The eight contemporary "control" coral records were stacked, by removing the mean of each record, to calculate an average record and the range of variability for the control population. The Great Palm Island record was normalized to the other colonies so that the means of the two records are equal over the period of unaltered skeleton from 1955 to 1970. Error bars are 1sd analytical reproducibility between replicates. MgCa was analysed twice; on subsamples before ("untreated") and after ("treated") cleaning treatments.

diagenesis. *Enmar et al.* [2000] found the colony's interstitial pore water Sr concentration and Sr/Ca was lower than open reef water. Similarly, *Lazar et al.* [2004] measured low U concentrations and U/Ca in pore waters. As reported by *Enmar et al.* [2000] and *Lazar et al.* [2004], secondary aragonite overgrowth could not be the only cause of the Sr and U deficits because the amount deposited was constrained by the observed alkalinity and enriched pore water Ca concentrations. *Lazar et al.* [2004] concluded that the living coral polyps had to be taking up U in order to deplete pore waters within the colony skeleton. However, the elevated Ca indicates dissolution was occurring, and the increased porewater Ca concentration relative to Sr and U, would result from the preferential leaching of Ca relative to the two trace elements.

4.2. Geochemical Impact of Secondary Aragonite on Coral Climate Tracers

[20] Secondary aragonite overgrowth causes artefacts in all the coral proxy-climate indicators examined: $\delta^{18}O$, $\delta^{13}C$, Sr/Ca, U/Ca, Mg/Ca, and density (Figure 4). It has been recognized for some time that coral precipitate their aragonitic skeletons out of equilibrium with seawater. Coral skeletons are depleted in Sr [*Buddemeier et al.*, 1981; *Swart*, 1981], U [*Meece and Benninger*, 1993; *Swart and Hubbard*, 1982; *Thompson and Livingston*, 1970], $\delta^{18}O$ and $\delta^{13}C$ [e.g., *McConnaughey*, 1989; *Weber and Woodhead*, 1970] relative to abiotic aragonite precipitated directly from seawater. The comparison between coral aragonite and abiotic aragonite for Mg is less clear because of the wide range of values reported for coral, but it is generally accepted that Mg is slightly enriched in coral aragonite [*Buddemeier et al.*, 1981]. This nonequilibrium behavior by coral explains the relative geochemical anomalies measured in the tracers for the secondary aragonite-contaminated samples (Figure 4b). Despite the offset between coral aragonite and abiotic secondary aragonite, the absolute $\delta^{13}C$, $\delta^{18}O$, and Mg/Ca values for the material containing secondary aragonite are within the spread of values obtained from various pristine coral (Figure 4a).

[21] The excellent agreement between the $\delta^{18}O$, Sr/Ca, and Mg/Ca SST reconstructions of the secondary aragonite contaminated coral (-1.6°C, -1.7°C, and -1.9°C, respectively) highlights the danger of using tracers replicated within a single coral to validate climate-proxy interpretations (Figure 5a). Although the apparent SST anomaly recorded by U/Ca in this study is suspiciously large (-2.8°C), the results of *Lazar et al.* [2004] show that this discrepancy can not be relied on as a warning indicator for diagenesis. *Lazar et al.* [2004] concluded the opposite, that U/Ca-SST reconstructions were more robust than Sr/Ca because the SSTA associated with secondary aragonite were significantly lower for U/Ca (-0.9°C) than Sr/Ca (-1.4°C).

4.3. Recommendations for Robust Coral Paleoclimate Reconstructions

[22] It is critical to screen out diagenetically altered coral material because it can still provide apparently realistic SST estimates, with these reconstructions well-reproduced within a colony by the alternative SST proxies. For this reason we propose that the coral paleoclimate community should no longer accept the pseudoreplication [*Hurlbert*, 1984] of various geochemical tracers within a colony as proof of the robustness of a coral-based SST reconstruction. Instead, the community needs to adopt other screening procedures as it has done with fossil coral samples where it is now accepted practice to screen for 100% aragonite composition by XRD and petrology to eliminate samples diagenetically altered by calcite overgrowth [e.g., *McGregor and Gagan*, 2003].

[23] We find that screening for secondary aragonite overgrowth is relatively simple and can occur prior to geochemical analysis by looking for (1) anomalous high density in X-ray images and in densitometry tracks, (2) mottled patches of high luminescence under UV light, followed by (3) positively identifying the presence of secondary aragonite by using SEM to observe overgrowth of sharply pointed acicular aragonite and infilling of pores.

[24] Early marine dissolution is not apparent from densitometry or X-ray images but can be identified visually using SEM by (1) exposure of fasciculi bundles and an etched appearance of the skeletal wall surface, (2) pitting or a melted appearance of individual crystals, (3) the loss of the granular microcrystalline aragonite surface coating.

[25] Dissolution is also readily detected in anomalies between replicated geochemical records from contemporary colonies. For these reasons the standard procedure to develop coral-based climate reconstructions has to involve the replication of records from different colonies as validation [e.g., *Lough*, 2004; *Hendy et al.*, 2002; *Linsley et al.*, 2006].

[26] This study also demonstrates that all coral material needs to be screened because postdepositional artefacts can occur in very recent coral skeleton. In the Great Palm core, secondary aragonite overgrowth occurred within a decade of the skeleton being laid down by the colony, whereas century-old skeleton was in pristine condition (Figure 3). This observation conflicts with models of secondary aragonite deposition that assume a continuously additive process with age [*Enmar et al.*, 2000].

4.4. Avoiding Colonies Susceptible to Diagenesis

[27] Understanding why this one particular coral colony out of nine specimens has zones of dissolution and secondary aragonite overgrowth would also improve screening. Microbial activity and decomposition of organic matter can lower the pH of pore water and cause porewaters to become undersaturated for aragonite [*Purser and Schroeder*, 1986], but there are no obvious signs why the particular zone in the Great Palm Island colony should be vulnerable to this process. In fact, the selective nature of the dissolution indicates that the porewaters are saturated in aragonite [*Constantz*, 1986]. Differences in the magnitude of diagenesis between coral species have been attributed to skeletal porosity [*Constantz*, 1986], and the low density and fast extension rate of the Great Palm Island colony's skeleton may have encouraged diagenesis by allowing greater percolation of water through skeleton than the other colonies in this study. The average density of the Great Palm Island colony (1.02 ± 0.05 g cm^{-3} y^{-1}) is lower than the typical *Porites* colony in the GBR (average density $1.17 \pm$

0.10 g cm^{-3} y^{-1}; range 0.98 to 1.39 g cm^{-3} y^{-1}; n = 35) [*Lough and Barnes*, 1997], while the extension rate is higher than average (18.9 ± 3.9 mm y^{-1} compared with all core average of 14.8 ± 3.2 and range from 8.8 to 21.7) [*Lough and Barnes*, 1997]. *Constantz* [1986] also observed that biogenic aragonite is significantly more susceptible to selective dissolution than marine cements and suggested that this reflected crystal growth rate related defects in the rapidly deposited biogenic aragonite. Coincidently, the fastest extension rate for the whole century-long Great Palm Island core is seen in the 15 years from 1965–1970 and 1975–1980 where the diagenesis is found. However, the powdered samples from the Great Palm Island colony were also noticeably more susceptible to dissolution that the other coral samples during sonication pretreatment and weak acid leaching required for Mg/Ca analysis. This indicates that the diagenesis is not simply the result of skeletal porosity but is related to smaller-scale vulnerabilities.

5. Conclusions

[28] The effect of skeletal dissolution on coral paleoclimate records has not been previously recognized. Dissolution, through incongruent leaching, causes cool SST artifacts in trace element ratios (Sr/Ca, U/Ca, and Mg/Ca) commonly measured in coral skeletons as paleotemperature tracers. Diagenesis, in the form of dissolution and secondary aragonite, can also occur extremely rapidly in very recent skeleton. It is important that coral material for paleoclimate reconstructions is screened for both dissolution and the presence of secondary mineral overgrowth. Poor replication of records between contemporary colonies and SEM imaging give the best indication of the presence of diagenetic artifacts, although secondary aragonite is also observed as high-density anomalies on X-ray images and bright mottling under UV light. We conclude that pseudoreplication [*Hurlbert*, 1984] of proxy tracers within a colony does not provide validation of SST reconstructions.

[29] **Acknowledgments.** E.J.H. is grateful to Peter Isdale, Bruce Parker, and Monty Devereux (AIMS) for collecting the coral samples and assistance from Heather Scott-Gagan, Joan Cowley, and Joe Cali in the ANU Stable Isotope Lab, Les Kinsley and Graham Mortimer in the ANU Isotope Geochemistry Lab, and Roger Heady at the ANU Electron Microscope Unit. This research has benefited greatly from the input of Chantal Alibert and Ian Fairchild. E.J.H. was supported by an Australian Postgraduate Award while at ANU and a Comer Abrupt Climate Postdoctoral Fellowship and NSF grant (OCE -0632134) while at Lamont Doherty Earth Observatory. Funding for the Mg/Ca analyses was provided by the Vetlessen Foundation.

References

Alibert, C., and M. T. McCulloch (1997), Strontium/calcium ratios in modern *Porites* corals from the Great Barrier Reef as a proxy for sea surface temperature: calibration of the thermometer and monitoring of ENSO, *Paleoceanography*, *12*, 345–365.

Allison, N. (1996), Comparative determinations of trace and minor elements in coral aragonite by ion microprobe analysis, with preliminary results from Phuket, southern Thailand, *Geochim. Cosmochim. Acta*, *60*, 3457–3470.

Amiel, A. J., G. M. Friedman, and D. S. Miller (1973), Distribution and nature of incorporation of trace elements in modern aragonitic corals, *Sedimentology*, *20*, 47–64.

Bar-Matthews, M., G. L. Wasserburg, and J. H. Chen (1993), Diagenesis of fossil coral skeletons: Correlation between trace elements, textures, and $^{234}U/^{238}U$, *Geochim. Cosmochim. Acta*, *57*, 257–276.

Boyle, E. A., and L. Keigwin (1985), Comparison of Atlantic and Pacific paleochemical records for the last 215,000 years: changes in deep ocean circulation and chemical inventories, *Earth Planet. Sci. Lett.*, *76*, 135–150.

Boyle, E. A., and Y. Rosenthal (1996), Chemical hydrography of the South Atlantic during the Last Glacial Maximum: Cd and $\delta^{13}C$, in *The South Atlantic: Present and Past Circulation*, edited by G. Wefer et al., pp. 423–443, Springer, New York.

Buddemeier, R. W., R. Schneider, and S. V. Smith (1981), The alkaline earth chemistry of corals, *Proc. Int Coral Reef Symp.*, *4*, 81–85.

Castellaro, C., B. Savary, A. Ribaud-Laurenti, B. Hamelin, L. Montaggioni, A. Juillet-Leclerc, and J. Recy (1999), Influence of marine diagenesis on geochemical records of $\delta^{18}O$, Sr/Ca and U/Ca in *Porites* skeleton, paper presented at Paleoceanology of Reefs and Carbonate Platforms: Miocene to Modern, ASF, Aix-en-Provence, France.

Constantz, B. R. (1986), The primary surface area of corals and variations in their suceptibility to diagenesis, in *Reef Diagenesis*, edited by J. H. Schroeder and B. H. Purser, pp. 53–76, Springer, Berlin.

Cuif, J.-P., and Y. Dauphin (2004), The environment recording unit in coral skeletons: structural and chemical evidences of a biochemically driven stepping-growth process in coral fibres, *Biogeosci. Disc.*, *1*, 625–658.

Enmar, R., M. Stein, M. Bar-Matthews, E. Sass, A. Katz, and B. Lazar (2000), Diagenesis in live corals from the Gulf of Aqaba. I. The effect on paleo-oceanography tracers, *Geochim. Cosmochim. Acta*, *64*, 3123–3132.

Fairchild, I. J., and J. A. Killawee (1995), Selective leaching in glacierized terrains and implications for retention of primary chemical signals in carbonate rocks, in *Water-Rock Interaction, Proceedings of the* 8th *International Symposium on Water-Rock Interaction - WRI-8*, pp. 79–82, A.A. Balkema, Rotterdam, Netherlands.

Gagan, M. K., L. K. Ayliffe, D. Hopley, J. A. Cali, G. E. Mortimer, J. Chappell, M. McCulloch, and M. J. Head (1998), Temperature and surface-ocean water balance of the mid-Holocene tropical western Pacific, *Science*, *279*, 1014–1018.

Gagan, M. K., E. J. Hendy, S. G. Haberle, and W. S. Hantoro (2004), Post-glacial evolution of the Indo-Pacific Warm Pool and El Niño-Southern Oscillation, *Quat. Int.*, *118–19*, 127–143.

Hendy, E. J., M. K. Gagan, C. A. Alibert, M. T. McCulloch, J. M. Lough, and P. J. Isdale (2002), Abrupt decrease in tropical Pacific sea surface salinity at end of Little Ice Age, *Science*, *295*, 1511–1514.

Hendy, E. J., M. K. Gagan, and J. M. Lough (2003), Chronological control of coral records using luminescent lines and evidence for non-stationary ENSO teleconnections in northeast Australia, *Holocene*, *13*, 187–199.

Hurlbert, S. H. (1984), Pseudoreplication and the design of ecological field experiments, *Ecol. Monogr.*, *54*, 187–211.

Lazar, B., R. Enmar, M. Schossberger, M. Bar-Matthews, L. Halicz, and M. Stein (2004), Diagenetic effects on the distribution of uranium in live and Holocene corals from the Gulf of Aqaba, *Geochim. Cosmochim. Acta*, *68*, 4583–4593.

Linsley, B. K., A. Kaplan, Y. Gouriou, J. Salinger, P. B. deMenocal, G. M. Wellington, and S. S. Howe (2006), Tracking the extent of the South Pacific Convergence Zone since the early 1600s, *Geochem. Geophys. Geosyst.*, *7*, Q05003, doi:10.1029/2005GC001115.

Lough, J. M. (2004), A strategy to improve the contribution of coral data to high-resolution paleoclimatology, *Palaeogeogr. Palaeoclimatol. Palaeoecol.*, *2004*, 115–143.

Lough, J. M., and D. J. Barnes (1997), Several centuries of variation in skeletal extension, density and calcification in massive *Porites* colonies from the Great Barrier Reef: A proxy from seawater temperature and a background of variability against which to identify unnatural change, *J. Exp. Mar. Biol. Ecol.*, *211*, 29–67.

Lough, J. M., and D. J. Barnes (2000), Environmental controls on growth of the massive coral Porites, *J. Exp. Mar. Biol. Ecol.*, *245*, 225–243.

Lough, J. M., D. J. Barnes, M. J. Devereux, B. J. Toblin, and S. Toblin (1999), Variability in growth characteristics of massive *Porites* on the Great Barrier Reef, *Tech. Rep. 28*, 95 pp.,

CRC Reef Research Centre, Townsville, Queensland, Australia.

McConnaughey, T. (1989), ^{13}C and ^{18}O isotopic disequilibrium in biological carbonates: I. Patterns, *Geochim. Cosmochim. Acta*, *53*, 151–162.

McGregor, H. V., and M. K. Gagan (2003), Diagenesis and geochemistry of *Porites* corals from Papua New Guinea: Implications for paleoclimate reconstruction, *Geochim. Cosmochim. Acta*, *67*, 2147–2156.

Meece, D. E., and L. K. Benninger (1993), The coprecipitation of Pu and other radionuclides with $CaCO_3$, *Geochim. Cosmochim. Acta*, *57*, 1447–1458.

Meibom, A., S. Mostefaoui, J.-P. Cuif, Y. Dauphin, F. Houlbreque, R. B. Dunbar, and B. R. Constantz (2007), Biological forcing controls the chemistry of reef-building coral skeleton, *Geophys. Res. Lett.*, *34*, L02601, doi:10.1029/2006GL028657.

Min, G. R., R. L. Edwards, F. W. Taylor, J. Recy, C. D. Gallup, and W. J. Beck (1995), Annual cycles of U/Ca in coral skeletons and U/Ca thermometry, *Geochim. Cosmochim. Acta*, *59*, 2025–2042.

Mitsuguchi, T., T. Uchida, E. Matsumoto, P. Isdale, and T. Kawana (2001), Variations in Mg/Ca, Na/Ca, and Sr/Ca ratios of coral skeletons with chemical treatments: implications for carbonate chemistry, *Geochim. Cosmochim. Acta*, *65*, 2865–2874.

Müller, A., M. K. Gagan, and M. McCulloch (2001), Early marine diagenesis in corals and geochemical consequences for paleoceanographic reconstructions, *Geophys. Res. Lett.*, *28*, 4471–4474.

Müller, A., M. K. Gagan, and J. M. Lough (2004), Effect of early marine diagenesis on coral reconstructions of surface-ocean $^{13}C/^{12}C$ and carbonate saturation state, *Global Biogeochem. Cycles*, *18*, GB1033, doi:10.1029/2003GB002112.

Plummer, L. N., E. Busenberg, P. D. Glynn, and A. E. Blum (1992), Dissolution of aragonite-strontianite solid solutions in nonstoichiometric Sr $(HCO_3)_2$-Ca $(HCO_3)_2$-CO_2-H_2O solution, *Geochim. Cosmochim. Acta*, *56*, 3045–3072.

Purser, B. H., and J. H. Schroeder (1986), The diagenesis of reefs: a brief review of our present understanding, in *Reef Diagenesis*, edited by J. H. Schroeder and B. H. Purser, pp. 424–446, Springer, Berlin.

Quinn, T. M., and F. W. Taylor (2006), SST artifacts in coral proxy records produced by early marine diagenesis in a modern coral from Rabaul, Papua New Guinea, *Geophys. Res. Lett.*, *33*, L04601, doi:10.1029/2005GL024972.

Schrag, D. P. (1999), Rapid analysis of high-precision Sr/Ca ratios in corals and other marine carbonates, *Paleoceanography*, *14*, 97–102.

Schroeder, J. H. (1969), Experimental dissolution of calcium, magnesium, and strontium from recent biogenic carbonates: a model for diagenesis, *J. Sediment. Petrol.*, *39*, 1057–1073.

Sinclair, D. J., L. Kinsley, and M. McCulloch (1998), High resolution analysis of trace elements in corals by laser ablation ICP-MS, *Geochim. Cosmochim. Acta*, *62*, 1889–1901.

Swart, P. K. (1981), The strontium, magnesium and sodium composition of recent scleractinian coral skeletons as standards for palaeoenvironmental analysis, *Palaeogeogr., Palaeoclimatol., Paleoecol.*, *34*, 115–136.

Swart, P. K., and J. A. Hubbard (1982), Uranium in scleractinian coral skeletons, *Coral Reefs*, *1*, 13–19.

Thompson, G., and H. D. Livingston (1970), Strontium and uranium concentrations in aragonite precipitated in some modern corals, *Earth Planet. Sci. Lett.*, *8*, 439–442.

Weber, J. N., and P. M. Woodhead (1970), Carbon and oxygen isotope fractionation in the skeletal carbonate of reef-building corals, *Chem. Geol.*, *6*, 93–117.

P. B. deMenocal, Lamont-Doherty Earth Observatory of Columbia University, Palisades, NY 10964, USA.

M. K. Gagan and M. McCulloch, Research School of Earth Sciences, Australian National University, Canberra, ACT 0200, Australia.

E. J. Hendy, Department of Earth Sciences, University of Bristol, Bristol BS8 1RJ, UK. (e.hendy@bristol.ac.uk)

J. M. Lough, Australian Institute of Marine Science, PMB3, Townsville MC, Queensland 4810, Australia.